ISBN: 978-3-95450-132-8 doi:10.18429/JACoW-IPAC2014-WEPME037

# MONTE CARLO SIMULATIONS OF SYNCHROTON RADIATION AND VACUUM PERFORMANCE OF THE MAX IV LIGHT SOURCE

M. Ady, R. Kersevan (CERN, Geneva, Switzerland), M. Grabski (MAX IV, Lund, Sweden)

*Abstract*

In the 3 GeV ring of MAX IV light source in Lund, Sweden, the intense synchrotron radiation (SR) distributed along the ring generates important thermal and vacuum effects. By means of a Monte Carlo simulation package, which is currently developed at CERN, both thermal and vacuum effects are quantitatively analysed, in particular near the crotch absorbers and the surrounding NEG-coated vacuum chambers. Using SynRad+, the beam trajectory of the upstream bending magnet is calculated; SR photons are generated and traced through the geometry until their absorption. This allows an analysis of the incident power density on the absorber, and to calculate the photon induced outgassing. The results are imported to Molflow+, a Monte Carlo vacuum simulator that works in the molecular flow regime, and the pressure in the vacuum system and the saturation length of the NEG coating are determined using iterations.

## INTRODUCTION

MAX IV is a new synchrotron light source facility being constructed in Lund, Sweden. The facility comprises of a 3.4 GeV linac, 1.5 GeV and 3 GeV storage rings and a short pulse facility. The 3 GeV ring (528 m in circumference) will be an ultra-low emittance ring (bare lattice emittance of 0.33 nm·rad) based on multi-bend achromat (MBA) magnet concept.

Due to the compact magnet design and small magnet aperture of 25 mm, the majority of the vacuum chambers are designed as circular tubes of 22 mm inside diameter and 1 mm wall thickness. Their specific conductance is only 1.3 l·m/s for $N_2$ at room temperature. To reduce pressure, all the conductance limited chambers are planned to be coated with non-evaporable getter (NEG) film of TiZrV. The coating is deposited by magnetron sputtering method that was developed at CERN and is used in other synchrotron light facilities around the world.

Each of the 20 vacuum achromats of the 3 GeV ring is equipped with three sputter ion pumps and one crotch absorber in the place where the electron and photon beams split. The synchrotron radiation fan between the two beams impinges on the crotch absorber. To cope with large outgassing at that position, one of the ion pumps is located directly below the absorber. The upstream keyhole profiled structure and the downstream beam chamber are NEG-coated starting from 6 cm from the ion pump chamber. The wall of that pump chamber is also coated.

In order to estimate the thermal load and to create detailed photodesorption maps on the vacuum chamber walls a recently improved Monte Carlo software package was used: Synrad+[1] simulates synchrotron radiation distribution from the upstream bending magnet and Molflow+[2] performs the pressure profile simulations inside the vacuum chamber.

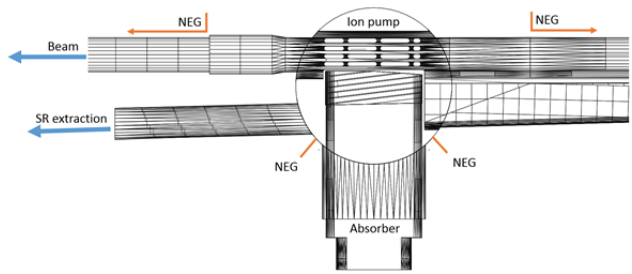


Figure 1: Top view of the vacuum chamber with the absorber.

One of the new features of the two programs is that the generated synchrotron radiation map in Synrad+ can be imported to Molflow+ and automatically converted to an outgassing map. This article describes the whole process which concludes in determining the pressure profile around the absorber.

## SYNCHROTRON RADIATION SIMULATION

The first calculation step is determining the absorbed SR power and flux on the chamber wall, which serves as base to calculate the thermal load and the dynamic outgassing. To achieve this, a CAD model describing the region around the absorber is imported to SynRad+. It consists of 8595 facets, the majority of them describing the pumping ports next to the absorber.

The dipole magnet (DIPm) 451 mm upstream of the modeled section has a 0.5 T average strength and 1.5° bending angle. In SynRad+, it is described as a *magnetic region* where the trajectory is calculated automatically from the beam energy, starting direction and the magnetic field.

Upon launching the simulation, virtual test photons are generated with uniformly distributed starting locations along the calculated beam path. Once their energy and starting direction is assigned, they are launched towards the system, each representing a given physical photon flux and power.

The ray-tracing algorithm finds collisions with the chamber wall, where depending on the incident angle and photon energy, a reflection probability is interpolated from material data [3]. It is used to decide if the virtual photon is absorbed or reflected. When reflection occurs, the reflection direction is perturbed by a simulated surface roughness. Photons are traced until absorption, when the algorithm reiterates by creating a new virtual photon.

ISBN: 978-3-95450-132-8 doi:10.18429/JACoW-IPAC2014-WEPME037

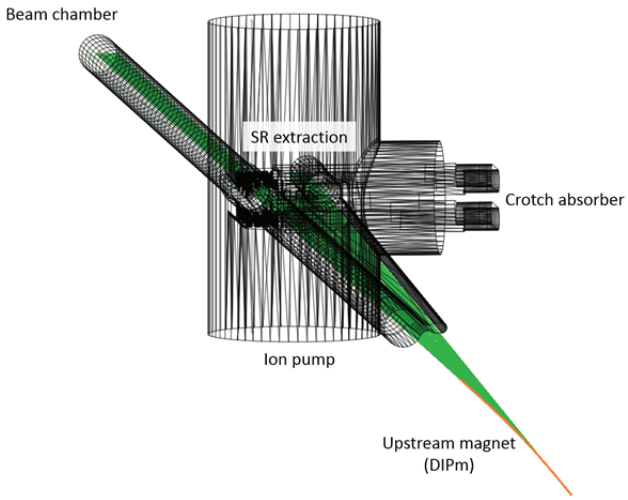


Figure 2: The dipole magnet and SR radiation schematics.

To determine the power and flux distribution, 5 million test photons were generated, representing the real flux of $4.2 \cdot 10^{18}$ photons/sec and power of 700.7 W generated by the magnet at the nominal current of 500 mA.

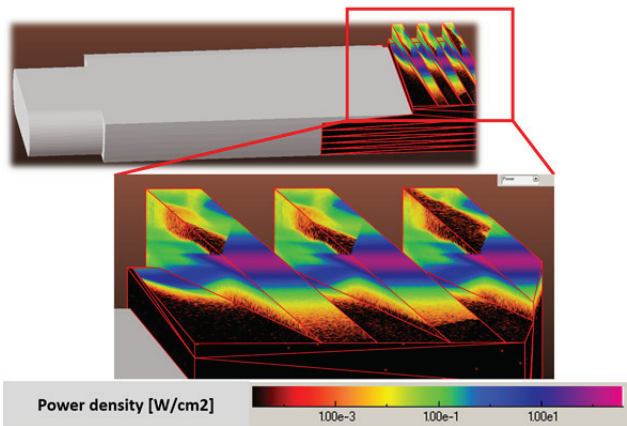


Figure 3: power density on the lower jaw of the absorber.

The absorber jaws receive 407 W of the SR power, with the highest power density of 6.1 W/mm$^2$, a value which is below the thermal limit for copper. A further 33 W is deposited on the outer wall of the downstream beam pipe, distributed on a meter-long distance thus causing negligible heating. The remaining power leaves the modeled region through the light and beam ports.

As for the photon flux, 50% is absorbed by the crotch absorber, approximately 40% leaves the region through the beam and SR extraction ports, and the rest is absorbed at various locations, typically after multiple reflections.

The highest SR flux density, corresponding to $6.8 \cdot 10^{17}$ photons/sec/cm$^2$ is also observed on the absorber's jaws.

## CONVERSION TO DYNAMIC OUTGASSING

Once the absorbed photon flux is determined, to convert it to dynamic outgassing, the photodesorption yield, i.e. the number of gas molecules that are released per incoming photon must be known.

This has been measured previously for several materials. In this paper measurements [4] for an oxygen free high conductivity copper chamber are used as it corresponds to the absorber's material.

The desorption yield depends on the absorbed photon dose (it decreases as the surface is conditioned by SR). However, the measurement data cannot be used directly as the photon dose is published using linear flux density (photons/m), whereas SynRad+ calculates surface density (photons/cm$^2$). The difference can be explained by the fact that Groebner et al. have measured the photodesorption by SR impinging on a 3.6 m long vacuum chamber wall with 11 mrad grazing angle. In our case, however, SR is absorbed by a short, complex crotch absorber geometry where the surface flux density is more meaningful.

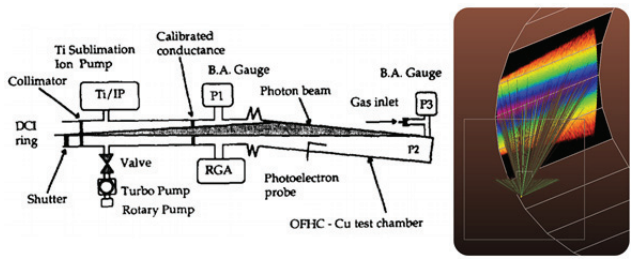


Figure 4: The original experiment schematics from Fig.1. of [4] and its simulation in SynRad+.

To be able to convert between the two dose types, the original experiment was recreated in Synrad+. The $10^{15}$ photons/sec flux of the original experiment was divided by the 3.6 m incidence length to obtain the linear density. In SynRad+, the simulated flux density has an average of $4 \cdot 10^{12}$ photons/sec/cm$^2$ on the approx. 1 cm high, 3.6m long slice of the tube where the majority of the SR is absorbed. Comparing the two quantities, it was deduced that 70 photons/m linear dose of the published data [4] corresponds to 1 photon/cm$^2$ surface dose simulated by Synrad+ on the irradiated parts.

Using this conversion factor, the desorption yield plots of the original article were digitized for the four most desorbed gases ($CH_4$, $H_2$, CO, $CO_2$) and exported in a format that can be used by Molflow+.

## VACUUM SIMULATIONS

Since file formats of Synrad+ and Molflow+ are compatible, the previously saved SR simulation can be opened directly for vacuum simulations. All SR data (magnetic regions, flux, material roughness) is removed so the vacuum chamber's pure geometry remains, therefore before starting the simulation the gas desorption and the pumping have to be added.

Four different vacuum simulations are performed – one for each gas. Taking advantage of the linear behavior of ultra-high vacuum systems, the partial pressures are summed at the conclusion.

To set up desorption, the flux data from the saved SR simulation is used (stored as *textures*, ie. absorbed flux densities assigned to locations on the chamber wall),

ISBN: 978-3-95450-132-8 doi:10.18429/JACoW-IPAC2014-WEPME037



along with the four molecule yield conversion files for each gas. To calculate the absorbed dose, the conditioning time is required for which the approximate value of 200 hours (100 Ah dose) was chosen.

Using these parameters, Molflow+ calculates the accumulated photon dose for every surface point, then interpolates the corresponding photon yield in the conversion files, then using the facet temperature and the ideal gas equation, converts the resulting outgassing flux from molecules/second to mbar·l/s, the default desorption unit. Performing the conversion, we obtain that the total outgassing from the four gases is $5 \cdot 10^{-7}$ mbar·l/s.

As for the pumping, the planned sputter ion pump under the absorber has a nominal pumping speed of 75 l/s for $H_2$ in the $10^{-9}$ mbar regime. However, for heavier gases it has to be adjusted as it is significantly lower.

A sticking factor of 0.1 is assigned to the three ports of the vacuum chamber (one upstream and two downstream). This represents that at those locations the gas is in equilibrium with the rest of the machine, except for an approximate 10% of the particles that leave the modeled region and are pumped elsewhere. The pumping properties of the NEG-coated sections are different for each gas, as described below.

### *Methane*

NEG does not pump methane [5], therefore its sticking is disabled in the simulation. However, on parts of the wall where SR is absorbed a local photo-induced conversion to other hydrocarbons [6-8] takes place, therefore it will be pumped by a linear speed of 10 l/s/m [9], which is set at those parts of the chamber wall and the absorber where SR flux is absorbed.

### *Hydrogen*

Hydrogen is pumped with a sticking factor of about 0.008 [5], and NEG saturation is not significant.

### *CO and $CO_2$*

Estimating pressure profile is more complex for these two gases. According to [5], initially they are pumped by NEG with a sticking factor of approx. 0.7, until they saturate the coating at an approximate molecule dose of $10^{15}$/cm$^2$, at which point the sticking is reduced to 0.002.

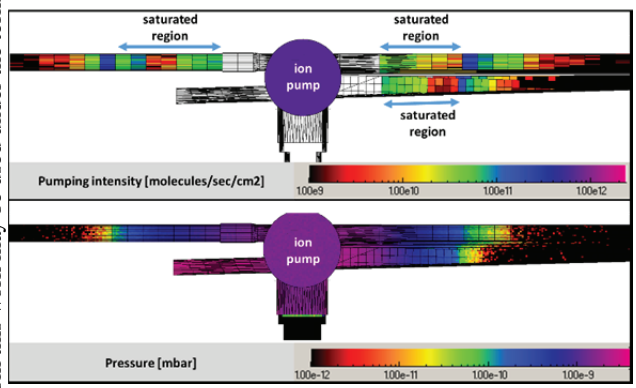


Figure 5: NEG saturation and its effect on pumping speed and pressure profile.

Therefore the simulation was performed in an iterative way: first the NEG was assumed unsaturated. The conditioning process was modelled in increasing time steps corresponding to an elapsed time of 10, 100 … 100.000, 720.000 seconds. At each time step, the simulation was stopped, then the number of molecules pumped by every NEG element up to that moment was determined.

If saturation occurred, based on interpolation from [5] a new, lower sticking factor was assigned locally for the next time slice, and the simulation resumed. In a total of 6 steps the 200 h conditioning time was reached, by which approximately 12 cm of the NEG film closest to the absorber reached saturation condition.

On Fig. 5 it can be seen that at the border of the saturated region, the first (unsaturated) NEG section pumps the most intensively, therefore reducing pressure in a steep drop.

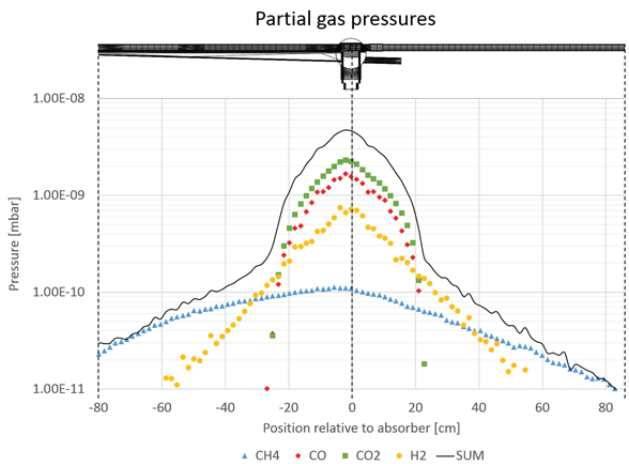


Figure 6: Partial gas pressures around the absorber.

The final pressure profile is shown in Fig.6. It can be seen that since the dynamic outgassing originates almost exclusively from the absorber surface, it introduces a locally elevated pressure in the $10^{-9}$ mbar region, which corresponds to a beam-gas scattering lifetime that is acceptable for the operation of MAX-IV.

## REFERENCES

[1] R. Kersevan, SYNRAD, a Monte Carlo synchrotron radiation ray-tracing program, Proceedings of the 1993 Particle Accelerator Conference, vol.5., p 3848-3850.

[2] R.Kersevan, J-L Pons, "Introduction to Molflow+", JVST A27 (2009), p1017-1023.

[3] B.L.Henke, E.M.Gullikson and J.C.Davis, X-Ray Interactions: Photoabsorption, Scattering, Transmission, and Reflection at E=50-30.000eV, Z=1-92, Center for X-Ray optics, lawrence Berkeley Laboratory, California 94720.

[4] O. Groebner, A.G. Mathewson, P.C. Marin; Gas desorption from an oxygen free high conductivity copper vacuum chamber by synchrotron radiation photons, J. Vac. Sci. Technol. A 12, 846 (1994).

[5] P. Chiggiato, P. C. Pinto - Ti-Zr-V non-evaporable getter films: from development to large scale production for the Large Hadron Collider, Thin Solid Films 515, 2 (2006).

ISBN: 978-3-95450-132-8 doi:10.18429/JACoW-IPAC2014-WEPME037

[6] V.V Anashin, I.R Collins, R.V Dostovalov, N.V Fedorov, A.A Krasnov, O.B Malyshev, V.L Ruzinov, Comparative study of photodesorption from TiZrV coated and uncoated stainless steel vacuum chambers, Vacuum, Volume 75, Issue 2, 12 July 2004, p. 155-159.
[7] V.V. Anashin, O.B. Malyshev, I.R. Collins, O. Gröbner, Photon-stimulated desorption and the effect of cracking of condensed molecules in a cryogenic vacuum system, Vacuum, Volume 60, Issues 1–2, January 2001, p. 15-24
[8] M. A. Gondal, Z. H. Yamani, A. Dastgeer, M. A. Ali, A. Arfaj, Photo-Conversion of Methane into Higher Hydrocarbons Using 355 NM Laser Radiation, Spectroscopy Letters Vol. 36, No. 4.
[9] R. Kersevan, CERN, unpublished measurement data at ESRF.